

## Superfluid Onset and Capillary Condensation

R.J. Lazarowich · P. Taborek

Received: 17 November 2006 / Revised: 10 May 2007 / Published online: 22 August 2007  
© Springer Science+Business Media, LLC 2007

**Abstract** We present experimental results on the superfluid onset of  $^4\text{He}$  adsorbed onto porous gold and evaporated  $\text{CaF}_2$  films grown on the electrodes of quartz microbalances (QCM). Adsorption and desorption isotherms were measured on the porous substrates in the range of 1.2 to 2.2 K. The isotherms were used to construct phase diagrams in the  $\mu-T$  plane showing hysteresis closure points and superfluid onsets. At low coverage, the superfluid onset showed both the abrupt frequency shift and dissipation peak characteristic of a conventional KT transition. Within hysteresis loops, a dissipation peak is observed, but the nearly discontinuous frequency shift is replaced by a smooth and gradual decoupling of the superfluid component as the coverage is increased. The gradual onset of superflow was analyzed using ideas from percolation theory.

**Keywords** Percolation theory · Capillary condensation · Superfluidity · QCM

**PACS** 67.70.+n · 64.70.Ja · 67.40.Hf · 67.40.Pm

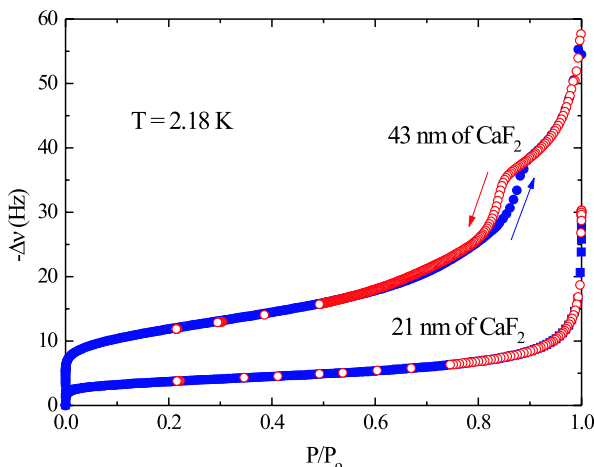
### 1 Introduction

The phase behavior of helium in porous materials has been studied in a wide range of materials using a variety of techniques [1–4]. The focus of this previous work has been either the low coverage, low temperature regime where the pores do not contain bulk fluid, or the regime near  $T_\lambda$  with full pores. Here we consider experimental data taken in the regime where capillary condensation and superfluid onset intersect; further details of this work are available [5].

---

R.J. Lazarowich (✉) · P. Taborek  
Department of Physics, University of California, Irvine, CA 92697, USA  
e-mail: lazarowi@chapman.edu

**Fig. 1** (Color online) Isotherms at 2.18 K on 21 nm and 43 nm of  $\text{CaF}_2$ . At 43 nm thickness, the first appearance of hysteresis takes place



Adsorption on the surfaces of a rough or porous substrate often involves capillary condensation, a hysteretic transition in which the dense liquid phase is stabilized in cracks and pores under thermodynamic conditions for which the bulk liquid phase would be unstable. In this experiment, we use QCMs with porous electrodes to study the interaction of superfluidity and capillary condensation. The QCMs are operated in diffusive contact with a large reservoir of vapor at a fixed temperature as the chemical potential offset from coexistence  $\Delta\mu$  is varied. Capillary condensation can be inferred by comparing forward and reverse adsorption isotherms [6].

Substrates of gold and calcium fluoride were created using previously developed techniques [7, 9]. Isotherms were used both to determine the structural properties such as surface area and porosity of the porous substrate and to study the phase behavior of helium in the porous media. All porous Au samples had similar features in their isotherms, but for  $\text{CaF}_2$ , there is a transition from a rough surface to a porous substrate that exhibits hysteresis. Hysteresis is first observed near 43 nm as shown in Fig. 1. As the thickness of  $\text{CaF}_2$  increases, the small hysteretic region becomes a broad loop as shown in Fig. 2. The nearly vertical feature at  $P/P_o = 0$  is due to the formation of strongly bound solid-like layers, and can be used to estimate the area of the pores. The closure point of the hysteresis loop, where all pores are assumed filled, can be used to estimate the pore volume. Both porous gold and calcium fluoride exhibit characteristics showing a natural distribution of pore size.

## 2 Superfluidity and Capillary Condensation

We have used the QCM to measure the conventional features of the KT transition, i.e. a frequency drop due to decoupling of the superfluid fraction, and a peak in the dissipation, for porous substrates; a typical example is shown in Fig. 2.

A noteworthy feature in the isotherms is the dissipation peak which marks the onset of superfluidity. We find that the relative size of the dissipation peak remains almost the same regardless of the substrate or the location in the isotherm of the

**Fig. 2** (Color online) Forward and reverse adsorption of helium in 95 nm of CaF<sub>2</sub> at  $T = 1.81$  K, showing  $\Delta\nu$  and the dissipation  $R$  as a function of reduced pressure. The frequency shift is very smooth through the superfluid transition, but the dissipation shows clear peaks. The dissipation is hysteretic in pressure, but the peaks which mark the transition correspond to the same frequency shift, indicating that the transition is determined by the coverage and not the pressure

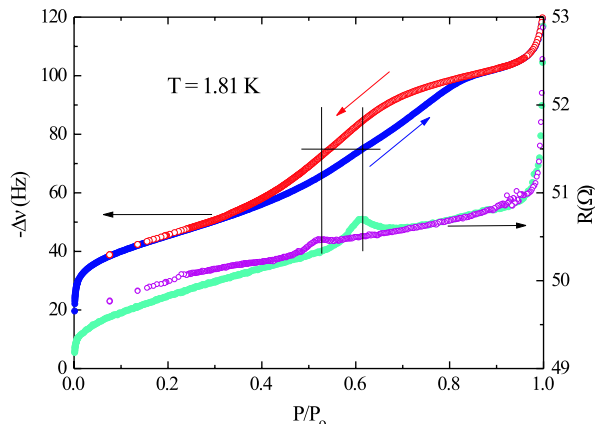
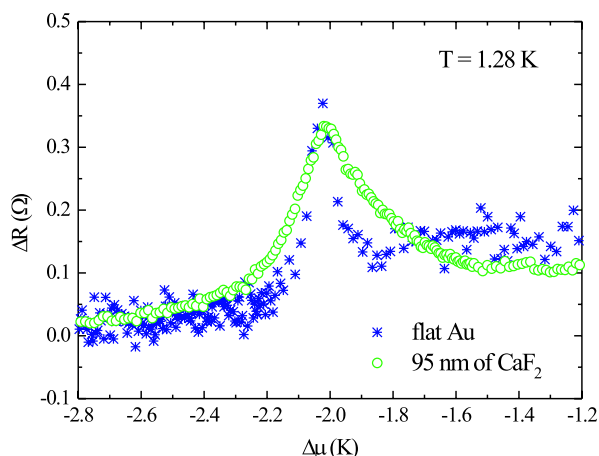


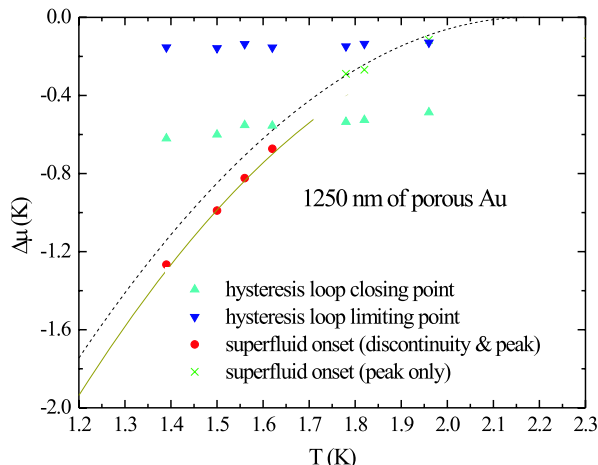
**Fig. 3** (Color online) Comparison of dissipation peaks due to the superfluid onset on flat Au and 95 nm of CaF<sub>2</sub> at  $T = 1.28$  K as a function of  $\Delta\mu$ . Remarkably, the dissipation peaks are of similar height even though there is 20 times the amount of fluid coupled to the CaF<sub>2</sub> substrate



transition, as shown in Fig. 3 which compares the dissipation peaks on a flat Au plate and in 95 nm of CaF<sub>2</sub>. In contrast, the frequency shift due to mass decoupling at the transition on porous materials depends critically on where in the hysteresis loop the transition takes place. In some cases, it became virtually impossible to detect the transition using only the frequency signal, as illustrated by the smooth  $\Delta\nu$  isotherm in Fig. 2. To construct complete phase diagrams for porous Au and CaF<sub>2</sub>, both the frequency shift and dissipation signatures of the superfluid onset were taken into account.

The main features of the porous gold phase diagram, shown in Fig. 4, are the approximately horizontal triangular points which mark the endpoints of the hysteresis loops, and the circles and crosses which mark superfluid onset. The dotted curve shows the relationship between the chemical potential and temperature expected for a flat gold substrate. Just as for flat substrates, superfluid onset occurs when the film thickness reaches the critical value, which can be accurately described using the theory of Saam and Cole [8].

**Fig. 4** (Color online)  $\Delta\mu$  versus  $T$  phase diagram for helium in a 1250 nm porous Au substrate. The dashed line represents the normal-superfluid boundary on flat Au. The superfluid onset in porous Au below capillary condensation has both KT features at the transition point and the curve passing through these points is based on theory



The phase diagram on  $\text{CaF}_2$  depends on the thickness of the porous substrate because of the transition from a rough to porous structure. On thin substrates of  $\text{CaF}_2$ , which do not have hysteresis, isotherms have both the frequency discontinuity and dissipation peak characteristic of a KT transition. The characteristics of the superfluid transition can be quantitatively explained by taking into account the increase in surface area of the substrate and the value of the superfluid drag coefficient [5].

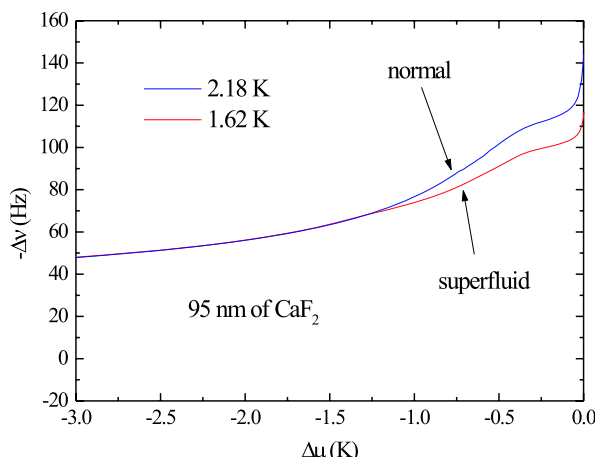
Isotherms on  $\text{CaF}_2$  substrates greater than 43 nm in thickness display hysteresis, and the superfluid transitions no longer have conventional KT features. Figure 2 presents a view of the transition region on the same  $\text{CaF}_2$  substrate, and shows the forward and reverse branches of the isotherm for both the frequency shift and the dissipation. The frequency shift has no hint of a discontinuity at the transition, but rather has a barely discernable and gradual change in slope. In contrast, the dissipation has clearly identifiable peaks at the transition. The separation of the peaks shows that the transition is hysteretic, but the transition occurs on both the adsorption and desorption branches at the same value of total helium coverage.

The nature of the transition can be more clearly seen by comparing two isotherms on the same substrates above and below  $T_\lambda$  as shown in Fig. 5. In the chemical potential range where the helium film is normal, the isotherms coincide, but for chemical potential values higher than  $\Delta\mu_c = -1.25$  K, the frequency shift for the 1.62 K isotherm is lower because the superfluid part decouples. The normal and superfluid isotherms deviate from each other in a smooth and continuous way, without the discontinuity or cusp expected from a 2D or 3D superfluid transition. The apparent superfluid fraction  $n_s$  grows as a power law with  $n_s \propto (\Delta\mu_c - \Delta\mu)^k$  where  $k$  is approximately 1.5. This type of power law growth is expected from a model in which isolated droplets in the medium percolate into a large cluster.

### 3 Conclusion

QCMs with porous electrodes have been used to study the phase behavior of helium in porous media. If superfluid onset occurs on the low coverage portion of the

**Fig. 5** (Color online) Forward isotherm on 95 nm of  $\text{CaF}_2$  at 2.18 K (blue) and 1.62 K (red). In the chemical potential range where the helium is normal, the isotherms coincide, but they separate at superfluid onset of the 1.62 K isotherm. The onset of superflow is characterized by a smooth, continuous separation from the normal isotherm



isotherm, the superfluid transition is a conventional 2D KT transition. The size and shape of the frequency shifts can be described using KT theory corrected for the increased area and the tortuosity of the substrate. As the temperature is increased, the coverage required for superfluid onset also rises and eventually enters the regime where the coverage is a hysteretic function. If superfluid onset occurs in this regime, the dissipation signature is unchanged from the low coverage behavior. This suggests that some aspect of the transition even in the hysteretic regime is still determined by the 2D criterion. In contrast, the frequency shift due to hydrodynamic mass decoupling no longer has a discontinuous step, but becomes smooth with a power law type behavior.

**Acknowledgements** This research is supported by NSF Grant No. DMR 0509685.

## References

1. N. Mulders, J.R. Beamish, Phys. Rev. Lett. **62**, 438 (1989)
2. H. Cho, V. Kotsubo, G.A. Williams, Can. J. Phys. **65**, 1532 (1987)
3. M.H.W. Chan, K.I. Blum, S.Q. Murphy, G.K.S. Wong, J.D. Reppy, Phys. Rev. Lett. **61**, 1950 (1988)
4. M.P. Lilly, R.B. Hallock, Phys. Rev. B **64**, 024516 (2001)
5. R.J. Lazarowich, P. Taborek, Phys. Rev. B **74**, 024512 (2006)
6. R.J. Lazarowich, P. Taborek, B.-Y. Yoo, N.V. Myung, J. Appl. Phys. **101**, 104909 (2007)
7. M. Hieda, A.C. Clark, M.H.W. Chan, J. Low Temp. Phys. **134**, 91 (2004)
8. W.F. Saam, M.W. Cole, Phys. Rev. B **11**, 1086 (1975)
9. D.R. Luhman, R.B. Hallock, Phys. Rev. Lett. **93**, 086106 (2004)